Folia Microbiologica (2020) 65:763–773
https://doi.org/10.1007/s12223-020-00790-9

ORIGINAL ARTICLE

Effect of the anti-inflammatory drug diclofenac on lipid composition of bacterial strain *Raoultella* sp. KDF8

Andrea Palyzová[1] · Helena Marešová[1] · Jiří Novák[1] · Jiří Zahradník[1] · Tomáš Řezanka[1]

Received: 27 January 2020 / Accepted: 8 April 2020 / Published online: 21 April 2020

Abstract

The strain *Raoultella* sp. KDF8 was cultivated on three sources of carbon and energy, glycerol, ethanol and diclofenac, for periods of time ranging from 24 to 72 h. Using thin-layer chromatography, nine classes of phospholipids were detected and the amount of phosphatidylethanolamine (PtdEtn) decreased with increasing cultivation time. Conversely, the ratio of phospholipids having three or four acyls (acyl-phosphatidylglycerol (APtdGro), *N*-acyl-PtdEtn (NAPtdEtn) and cardiolipin (Ptd_2Gro) increased during cultivation. GC-MS analysis showed that the percentage of fatty acids containing a cyclopropane ring increased almost tenfold whereas the amount of fatty acids bearing even-numbered chains dropped to less than one-third after 24 h and 72 h in cultures on glycerol and diclofenac, respectively. Shotgun analysis showed significant changes in the representation of molecular species of phospholipids. For instance, there was a 36-fold change in the ratio of 16:1/16:1/16:1-APtdGro to c17:0/c17:0/c17:0-APtdGro and a 12-fold ratio change for 16:1/16:1/16:1-NAPtdEtn to c17:0/c17:0/c17:0-NAPtdEtn; the Ptd_2Gro ratio of 16:1 to c17:0 acids equalled 1750. Our results show that the bacteria overcome destabilization of the inner cytoplasmic cell membrane and a bacterial outer membrane by altering the geometric arrangement of acyl chains, i.e. switching from monounsaturated to cyclopropane fatty acids (16:1 versus c17:0).

Introduction

Some microorganisms exposed to long-term selection pressure caused by hazardous pollutants develop a series of effective mechanisms in order to survive under adverse conditions. These adaptation mechanisms allow them to reduce the negative impact of these environmental substances. The bacterial surface structures create a selective barrier between the inside and outside of the cell, and many adaptive mechanisms are therefore focused on the flexibility of these cellular membranes.

To understand membrane functions, it is important to know the qualitative and quantitative lipid composition; this can be achieved by lipidomic analysis. Two basic techniques are used in lipidomic analysis. The first involves liquid chromatography/mass spectrometry (LC-MS) analysis (Knittelfelder et al. 2014) and the other involves the direct infusion of sample(s) into a mass spectrometer, also known as "shotgun lipidomics" (Han and Gross 2003). Shotgun lipidomics uses mainly electrospray ionization mass spectrometry (ESI/MS) without the assistance of chromatographic separations to investigate the biological functions and/or the importance and changes of lipids during cellular metabolism.

The accumulation of newly emerging pollutants such as active pharmaceutical ingredients and their metabolites in the aquatic environment has recently become a serious problem. One of these micropollutants is diclofenac (DCF; 2-(2′,6′-dichloranilino)phenyl acetic acid) belonging to the group of drugs known as nonsteroidal anti-inflammatory drugs that are used to treat pain and inflammatory diseases. The microbial co-metabolism or biotransformation of DCF have been intensively studied (Moreira et al. 2018; Palyzová et al. 2019), but many important aspects are still missing. Its degradation by manganese oxidation bacterium, i.e. *Pseudomonas putida* (Meerburg et al. 2012) has been described. In addition, the pure bacterial strain *Raoultella* sp. DD4 exhibited resistance to DCF and was able to biotransform it for 28 days (Domaradzka et al. 2016). Enhanced elimination of several pharmaceutical residues

Electronic supplementary material The online version of this article (https://doi.org/10.1007/s12223-020-00790-9) contains supplementary material, which is available to authorized users.

✉ Tomáš Řezanka
rezanka@biomed.cas.cz

[1] Institute of Microbiology, Czech Academy of Sciences, Vídeňská 1083, 142 20 Prague 4, Czech Republic

poorly removed by the CAS treatment (e.g. mefenamic acid, indomethacin, diclofenac, propyphenazone, pravastatin, gemfibrozil) was observed in pilot-scale membrane bioreactors (Radjenovic et al. 2009).

Since the membranes are the primary target of pollutants, most of the adaptive mechanisms henceforth revealed are likely related to the maintenance of membrane fluidity and lipid-phase stability. These processes can be modulated by altering the lipid composition of the membrane. To understand the contribution of membrane lipid composition to the functionality of membranes, comprehensive structural and quantitative information on the lipidomics is essential. Detailed lipidomic profiling using electrospray ionization (ESI) showed remarkable changes in the composition of phospholipids (phosphatidylethanolamine (PtdEtn), phosphatidylglycerol (PtdGro) and phosphatidylcholine (PtdCho)) produced by the gram-negative bacterium *Pseudomonas proteolytica* (Bernat et al. 2014). Liquid chromatography coupled with the tandem mass spectrometry (LC-MS/MS) technique revealed modifications in the ratio of PtdCho/PtdEtn and PtdEtn/PtdGro when *P. proteolytica* was cultivated with tributyltin. In another paper, the authors reported on altered lipid composition of *Escherichia coli* when grown in the presence of ethanol, pentobarbital and chlorpromazine (Ingram et al. 1978). Compared to the control culture in a complex medium, in the presence of different carbon sources, the palmitoleic acid (16:1) content declined, while odd-numbered C17 and C19 fatty acids (FA) were identified in the culture with chlorpromazine. In the case of phospholipids (PL), all three-carbon sources had the same effect; the percentage of PtdEtn was decreased while that of cardiolipin (Ptd_2Gro) and PtdGro increased. *E. coli* cultured in a medium containing glucose as a carbon source and supplemented with ethanol showed that the composition of Ptd_2Gro and PtdGro increased whereas the content of PtdEtn and lyso-PtdEtn decreased (Ingram 1977). A similar effect on FA content was found with palmitic (16:0) and 16:1 FA after adding ethanol to the media. The content of both acids in both PtdGro and PtdEtn decreased.

Segura et al. (1999) reported that the change in the composition of ester-bound FA in the bacterial membrane lipid bilayers and thus the regulation of membrane fluidity is a consequence of the cis/trans isomerization of FA as a short-term reaction to the solvent and the change in the ratio of saturated and unsaturated fatty acids as a long-term reaction. There is also an increase in the saturation of FA in membrane phospholipids in the presence of organic compounds (Heipieper et al. 2003). Aromatic compounds of the benzene, biphenyl, phenol, toluene, etc. type are accumulated in the membrane bilayer, i.e. acyls of FA, which results in an effect on membrane fluidity. Bacteria therefore seek to prevent their penetration by increasing membrane stiffness (Duldhardt et al. 2010). The presence of toxic organic compounds stimulates the biosynthesis of FA with cyclopropane rings, e.g. in gram-negative bacteria (Shabala and Ross 2008). Perly et al. (1985) stated that the low content of cyclo FA in the cell membrane can alter the stereochemistry of phospholipid acyls.

The present study was aimed at characterizing the cellular membrane lipid composition of the gram-negative bacterium *Raoultella* sp. KDF8 cultivated with DCF in order to elucidate cell adaptation to the organic micropollutants as substrates. This knowledge could provide insights into the understanding of how bacterial cells counteract the effect of organic pollutants on physiological processes, allowing them to survive in a DCF-contaminated environment. The study of these cell adaptations may help in selecting bacterial strains for bioremediation.

Materials and methods

Chemicals and materials

Standards of 2-((2,6-dichlorophenyl)amino)phenylacetic acid sodium salt (DCF), 1′,3′-bis(1,2-dimyristoyl-*sn*-glycero-3-phospho)-glycerol (14:0/14:0/14:0/14:0-Ptd_2Gro), 1,2-dipalmitoyl-*sn*-glycero-3-phospho-(1′-myo-inositol) (16:0/16:0-PtdIns), 1,2-dimyristoyl-*sn*-glycero-3-phospho-L-serine (14:0/14:0-PtdSer), 1,2-dimyristoyl-*sn*-glycero-3-phospho-(1′-rac-glycerol) (14:0/14:0-PtdGro), 1,2-dimyristoyl-*sn*-glycero-3-phosphoethanolamine (14:0/14:0-PtdEtn), 1,2-dimyristoyl-*sn*-glycero-3-phosphatidic acid (14:0/14:0-PtdOH), 1,2-dimyristoyl-*sn*-glycero-3-phosphocholine (14:0/14:0-PtdCho), and *N*-acyl-phosphatidylethanolamine (*N*-acyl-PtdEtn) from soy beans were purchased from Sigma-Aldrich (St. Louis, MO, USA). The solvent ethanol needed for the stock solutions of the DCF compounds (in concentrations of 1 g/L) was obtained from Thermo Fisher Scientific (San Jose, CA, USA). The other chemicals and ingredients used in the analysis were of high analytical grade and were obtained from Merck (Darmstadt, Germany).

Microorganism and culture conditions

The strain *Raoultella* sp. KDF8 (deposited at the CCM Collection, Czech Republic under accession number 8678) is a bacterium isolated from a polluted soil and subjected to chemical mutagenesis and capable of utilizing and removing DCF with high efficiency (Palyzová et al. 2018; Palyzová et al. 2019). The culture was grown in Luria-Bertani (LB) medium (per L: 10 g tryptone, 5 g yeast extract and 10 g NaCl) and the basal salts broth medium (BSB; per L: 0.1 g NaCl, 1.03 g K_2HPO_4, 0.75 g KH_2PO_4, 1 g NH_4Cl) supplemented with trace elements (BSBTE; per L: 200 mg $MgSO_4 \cdot 7H_2O$, 10 mg $CaCl_2 \cdot 2H_2O$, 6.6 mg $ZnSO_4 \cdot 7H_2O$, 0.17 mg $MnSO_4 \cdot 4H_2O$, 1.5 mg $FeSO_4 \cdot 7H_2O$, 0.48 mg $CoCl_2 \cdot 6H_2O$,

0.47 mg $CuSO_4 \cdot 5H_2O$, and 0.45 mg $Na_2MoO_4 \cdot 2H_2O$), respectively.

The pre-inoculum culture was grown in 100 mL of a LB medium (500-mL culture flask), on an orbital shaker (200 rpm) for 24 h at 28 °C. For the lipidomic study, the strain KDF8 was grown in 100 mL of BSBTE medium (500-mL culture flask) supplemented with either 2 g/L of glycerol (growth for 24 h), 1% ethanol (growth for 48 h) or 1 g/L DCF (growth for 72 h) on an orbital shaker (200 rpm) at 28 °C. DCF was added from stock solutions (1 g of analgesic dissolved in 10 mL of pure ethanol). A 1% inoculum was used to start the cultures.

Isolation of lipids

The lipids in the lyophilized biomass were extracted with a chloroform/methanol mixture according to Bligh and Dyer (1959). The extracts of total lipids were applied to the SPE sorbent cartridge (Sep-Pak Vac Silica cartridge 35cc; Waters, Milford, MA, USA), and non-polar lipids were subsequently eluted from the cartridge with 40 mL of chloroform-methanol in the volume ratio of 9:1. Polar lipids were eluted by a mixture of 50 mL of methanol acidified with 0.1% formic acid. The eluate of polar lipids was evaporated, and the oil samples were further hydrolysed.

Fatty acid methyl esters (FAME) analysis

Analysis of fatty acids in the form of methyl esters (FAME) was described previously (Dembitsky et al. 1992; Vancura et al. 1988). Fatty acids after hydrolysis of total lipids (2 mol/L HCl, 100 °C, 2.5 h) were extracted with hexane, methylated with 10% (w/v) methanolic BF_3 (80 °C, 10 min) and analysed by gas chromatography mass spectrometry (GC-MS). GC-MS of the FAME mixture was done on a Finnigan 1020 B in EI mode. The split/splitless injection port was maintained at 100 °C, and a fused silica capillary column (Supelcowax 10; 60 m × 0.25 mm i.d., 0.25 mm film thickness; Supelco, Munich, Germany) was used. A gradient of the temperature programming starting at 100 °C for 1 min with a ramp of 20 °C/min to 160 °C and another ramp of 15 °C/min to 220 °C with an 1-min hold at 220 °C was applied for the separation of FAME. The carrier gas was helium at a linear velocity of 60 cm/s. Compounds were identified by mass spectrometry in the SCAN mode using a mass interval ranging from 50 to 500 m/z. The structures of FAME were confirmed by comparing retention times and the fragmentation patterns with those of the standard FAME (Sigma-Aldrich).

TLC separation

The total polar lipids were subjected to preparative TLC (PLC silica gel 60 F254, 2 mm × 20 × 20 cm, Merck; chloroform/methanol/20% ammonium/water—90:70:4:16 (by vol.)). Visualization was carried out by dipping the plates in a mixture of 0.1% orcinol and 15% H_2SO_4 in ethanol followed by heating. For quantification, the developed chromatogram was scanned (by TLC scanner CS-930, Shimadzu, Columbia, MD, USA) in absorbance mode at 225 nm. The signals from the scanner were collected by Data Recorder DR-2 (Shimadzu) and were integrated and calculated using Statistica 9 software (StatSoft, Prague, Czech Republic), see Fig. 1S.

Shotgun analysis

An LTQ-Orbitrap Velos mass spectrometer (Thermo Fisher Scientific) was operated in negative ionization mode. The MS scan range was performed within a window between 200 and 2000 m/z, the mass resolution was set to 105,000 and the ion spray voltage was set at − 2.5 kV. The negative ionization mode used the following parameters: sheath gas flow, 18 arbitrary units (AU); auxiliary gas flow, 7 AU; ion source temperature, 250 °C; capillary temperature, 230 °C; capillary voltage, 50 V; and tube lens voltage, 170 V. Helium was used as a collision gas for collision-induced dissociation (CID) experiments. The CID normalization energy of 35% was used for the fragmentation of parent ions. The calibration of the MS spectrometer was conducted with the use of a Pierce LTQ Orbitrap negative ion calibration solution (Thermo Fisher Scientific). The internal lock mass was used in mass spectra acquisition, i.e. 255.2330 m/z $[M\text{-}H]^-$ palmitic acid in the negative ESI. The mass accuracy was better than 2 ppm. The chemical structure of the compounds was confirmed with the help of the spectral database LIPID MAPS® Lipidomics Gateway (http://www.lipidmaps.org/) and the CycloBranch programme (Novak et al. 2017).

Statistical analysis

Statistically significant differences between treatments and the control were computed by ANOVA (analysis of variance) or by ALSCAL (principal component analysis (PCA)) which produces a two-dimensional nonmetric Euclidean multidimensional scaling solution by using the IBM SPSS Statistics, version 26 software (IBM, USA).

Results

Cultivation and semi-quantification of phospholipids

Phospholipids were separated by TLC and nine bands were detected with Rf values 0.33 (PtdOH), 0.35 (PtdIns), 0.39 (PtdSer), 0.42 (PtdCho), 0.47 (PtdEtn), 0.57 (PtdGro), 0.72 (Ptd_2Gro), 0.79 (*N*-acyl-PtdEtn), and 0.82 acyl-phosphatidylglycerol (acyl-PtdGro), which were identified

by comparison with commercially obtained standards. TLC analysis revealed differences between cultivations of the strain KDF8 in terms of the growth phase of the culture and carbon source. The major phospholipid PtdEtn was detected in all samples. The relative content of PtdEtn decreased by the cultivation time and in response to the changes of the carbon source. The amounts of PtdEtn were the highest during the cultivation supplemented with glycerol as a carbon source and energy. Conversely, the content of phospholipids having three or four acyl chains in the molecule, i.e. *N*-acyl-PtdEtn, acyl-PtdGro and Ptd_2Gro, increased.

Analysis of cell membrane fatty acid composition in *Raoultella*

The identification of the fatty acid profile in different cultivations of the strain KDF8 was performed using the GC-MS method. The results are shown in Table 1. Based on the analyses, significant differences were found between two cultivations at the stationary growth phase, i.e. 24 h on glycerol and 72 h on DCF. While the content of odd- and even-numbered monounsaturated FA did not truly change, a dramatic shift occurred mainly in even-numbered FA and especially in cyclo FA. In two boundary cultures, the cyclo FA content increased almost tenfold while the content of even-chain FA decreased to less than one-third. Additionally, the ratio of the two major monoenoic FA, i.e. palmitoleic and oleic acids, also changed. These results suggest that cyclo FA are strongly involved in membrane fatty acid adaptation mechanisms in bacteria grown in the presence of DCF used as a carbon source.

Principal component analysis (PCA)

Figures 1 and 2 have several findings. First, it is apparent that the differences in FAs between different assays of the same sample, designated _1, _2 and _3, are negligible. The same conclusions can be drawn from the data in Tables 1 and 2. It is evident that in the case of glycerol, the effect of a different carbon source has already been demonstrated after 24 h of cultivation. In the case of using ethanol and a solution of DCF in ethanol as a carbon source, the effect at 24 h has not yet been observed. This is because ethanol is better utilized by cells than DCF. However, after utilization of ethanol, DCF begins to be utilized and therefore the FAs content of cultivation with ethanol and DCF shows a significant difference in the 48th h. The two clusters, i.e. Et48 and DCF48, are clearly separated. The last cluster, which consists of FAs analyses from the 72-h cultivation with DCF, is also clearly separated. It can be concluded that there are clear changes in the FAs content due to the different metabolism of the three types of carbon sources, i.e. glycerol, ethanol and DCF. Thus, it was unambiguously confirmed that DCF affects the FAs content of cell membranes.

In the case of molecular species of phospholipids analysis, the results of the statistical analysis shown in Fig. 2 were similar. Cluster G24, i.e. the cultivation of cells on glycerol and the analysis of phospholipids, showed that the content of molecular species is completely different from cultivations on other carbon sources. In the case of ethanol, the analysis results at 24 and 48 h are similar. This is probably due to the fact that, unlike the FAs analysis, the contribution of polar heads of phospholipids has to be taken into account in the analysis of

Table 1 Identified fatty acids (relative percentage) during cultivations of *Raoultella* sp. KDF8 at 24-h intervals

Fatty acid	24 G[a]	24 Et[a]	48 Et	24 DCF[a]	48 DCF	72 DCF
13:0	0.9 ± 0.2[b]	1.2 ± 0.3	1.7 ± 0.4	1.0 ± 0.3	0.9 ± 0.3	0.7 ± 0.2
14:0	1.9 ± 0.3	3.0 ± 0.4	3.4 ± 0.5	3.4 ± 0.4	2.2 ± 0.4	2.8 ± 0.4
15:0	0.4 ± 0.1	0.5 ± 0.2	0.6 ± 0.2	0.5 ± 0.1	0.7 ± 0.2	0.8 ± 0.3
16:1w7	32.7 ± 1.4	16.0 ± 0.9	26.8 ± 1.9	16.2 ± 1.2	18.4 ± 1.3	23.7 ± 1.3
16:0	30.1 ± 0.9	34.6 ± 1.5	11.9 ± 0.9	34.7 ± 1.0	22.1 ± 1.1	4.8 ± 0.7
c17:0	3.9 ± 0.4	20.2 ± 1.7	19.8 ± 1.3	20.4 ± 1.5	26.9 ± 1.3	30.8 ± 1.4
17:0	0.3 ± 0.2	0.2 ± 0.1	0.4 ± 0.2	0.2 ± 0.1	0.4 ± 0.2	0.5 ± 0.2
18:1w9	28.6 ± 1.7	20.8 ± 0.8	31.9 ± 1.1	21.0 ± 1.6	24.8 ± 1.0	31.4 ± 1.6
18:0	0.9 ± 0.2	2.3 ± 0.5	2.4 ± 0.6	1.0 ± 0.2	1.2 ± 0.3	1.5 ± 0.4
c19:0	0.3 ± 0.1	1.2 ± 0.6	1.1 ± 0.4	1.6 ± 0.4	2.4 ± 0.4	3.0 ± 0.5
Odd FA	1.6	1.9	2.7	1.7	2.0	2.0
Even FA	32.9	39.9	17.7	39.1	25.5	9.1
Monounsat. FA	61.3	36.8	58.7	37.2	43.2	55.1
Cyclo FA	4.2	21.4	20.9	22.0	29.3	33.8
Ratio 16:1/18:1	1.14	0.77	0.84	0.77	0.74	0.75

[a] Et, ethanol; G, glycerol; DCF, diclofenac

[b] Mean ± S.D. from three measurements

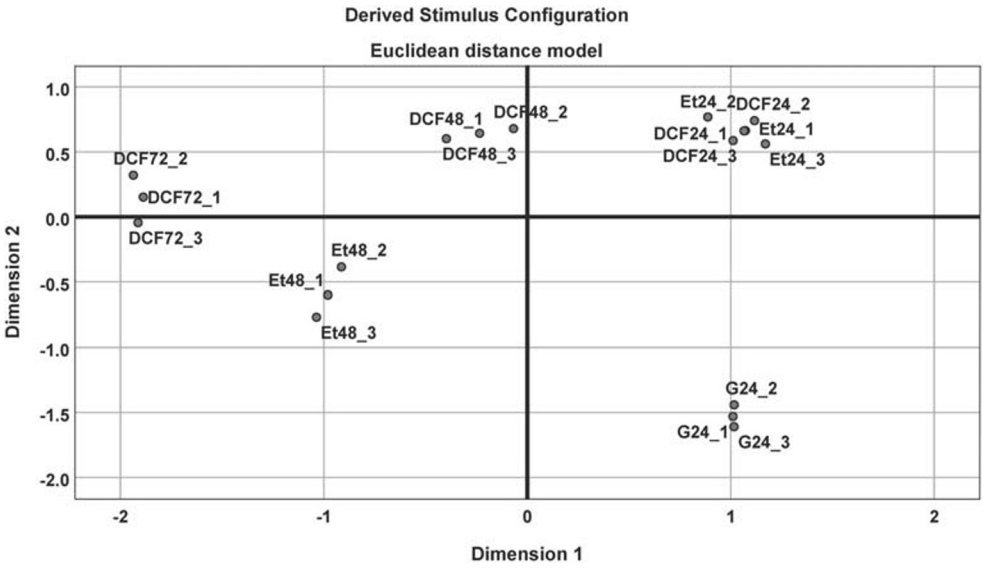

Fig. 1 Grouping of fatty acids contained in cultures grown in three different carbon sources using the ALSCAL procedure of SPSS software

molecular species of phospholipids. The results of cultivation with DCF differ in all three cases (24, 48 and 72 h). All three clusters are clearly separated and confirm that DCF has an influence on the representation of molecular species of phospholipids and thus on cell metabolism. Based on PCA, see Fig. 1 where the results of FAs analysis of bacterial culture after 24 h on both diclofenac and ethanol form a single cluster, it can be assumed that in the early phase of cultivation, there are no major changes in the content of fatty acids by diclofenac degradation products.

Analysis of phospholipids by tandem MS

Phospholipids contained in cells of the strain *Raoultella* sp. KDF8 were identified based on the tandem mass spectra obtained in the negative ESI. These mass spectra were used to characterize the structure of each class of phospholipids, as well as the structure of their molecular species including regioisomers. In the negative ESI tandem mass spectrum of the phospholipids, the deprotonated molecular ion $[M\text{-}H]^-$ is fragmented to form three major fragments, the first of which includes the ions resulting from the neutral loss of free carboxylic acid $[M\text{-}H\text{-}RCOOH]^-$, the second includes the $[M\text{-}H\text{-}R'CH{=}C{=}O]^-$ ions representing a neutral loss of the acyl group in the form of ketene, and the third is a carboxylate anion ($[RCOO]^-$). The identification of regioisomers that differ in the glycerol backbone acyl groups in *sn*-1 or *sn*-2 positions can be performed based on the relative intensities of the $[M\text{-}H\text{-}R'CH{=}C{=}O]^-$ type ions and comparing the relative abundance of these ions, see below.

The analysis of commonly occurring phospholipids, i.e. PtdOH, PtdSer, PtdEtn, PtdIns, PtdCho, PtdGro and

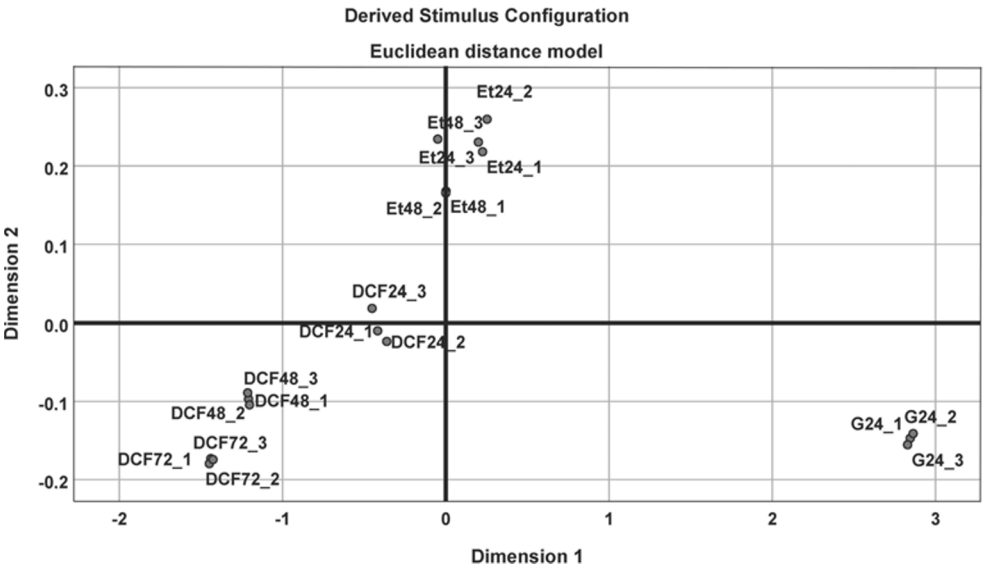

Fig. 2 Grouping of molecular species of phospholipids using the ALSCAL procedure of SPSS software

Table 2 Comparison of phospholipid composition of *Raoultella* sp. KDF8 exposed to DCF up to 72 h of incubation at 24-h intervals

m/z	CN/ dB	Class	Mol spec	24 G[a]	24 Et[a]	48 Et	24 DCF[a]	48 DCF	72 DCF	72DCF/ 24G
953.6852	48:3	APtdGro	16:1/16:1/16:1[b]	3.58 ± 0.14[c]	2.83 ± 0.47	2.09 ± 0.34	2.13 ± 0.34	1.67 ± 0.25	1.46 ± 0.78	0.41
967.7010	49:3	APtdGro	16:1/16:1/c17:0	1.32 ± 0.11	1.87 ± 0.51	1.96 ± 0.29	2.39 ± 0.27	2.41 ± 0.43	2.50 ± 0.57	1.89
983.7324	50:2	APtdGro	16:1/17:0/c17:0	0.33 ± 0.08	1.33 ± 0.39	1.45 ± 0.25	2.56 ± 0.41	2.87 ± 0.36	3.16 ± 0.61	9.58
995.7324	51:3	APtdGro	c17:0/c17:0/c17:0	0.26 ± 0.09	1.42 ± 0.42	1.58 ± 0.27	2.81 ± 0.36	3.09 ± 0.31	3.90 ± 0.82	15.00
1345.9184	64:3	Ptd_2Gro	16:0/16:1/16:1/16:1	11.05 ± 1.24	7.45 ± 1.08	6.58 ± 0.74	3.05 ± 0.24	2.47 ± 0.24	1.34 ± 0.18	0.12
1357.9176	65:4	Ptd_2Gro	16:1/16:1/16:1/c17:0	1.43 ± 0.32	2.17 ± 0.57	2.18 ± 0.64	3.14 ± 0.31	3.21 ± 0.28	3.38 ± 0.94	2.36
1371.9332	66:4	Ptd_2Gro	16:1/16:1/c17:0/c17:0	0.17 ± 0.07	2.12 ± 0.63	2.56 ± 0.57	3.41 ± 0.42	3.58 ± 0.39	4.00 ± 0.67	23.53
1385.9488	67:4	Ptd_2Gro	16:1/c17:0/c17:0/c17:0	0.15 ± 0.90	1.61 ± 0.45	1.89 ± 0.31	3.80 ± 0.47	3.99 ± 0.74	4.05 ± 0.85	27.00
1399.9644	68:4	Ptd_2Gro	c17:0/c17:0/c17:0/c17:0	0.03 ± 0.03	2.16 ± 0.48	2.32 ± 0.30	5.01 ± 0.39	5.13 ± 0.61	6.37 ± 0.39	212.33
922.6906	48:3	NAPtdEtn	16:1/16:1/16:1	4.24 ± 1.41	2.87 ± 0.29	2.66 ± 0.26	2.09 ± 0.27	1.88 ± 0.42	1.79 ± 0.32	0.42
936.7064	49:3	NAPtdEtn	16:1/16:1/c17:0	3.21 ± 0.98	3.45 ± 0.49	3.53 ± 0.47	4.02 ± 0.31	4.12 ± 0.33	4.37 ± 0.57	1.36
950.7219	50:3	NAPtdEtn	16:1/c17:0/c17:0	2.67 ± 1.04	4.67 ± 0.65	5.11 ± 0.43	7.16 ± 0.84	7.98 ± 0.76	8.14 ± 0.62	3.05
964.7378	51:3	NAPtdEtn	c17:0/c17:0/c17:0	1.83 ± 0.65	5.15 ± 0.57	5.90 ± 0.51	8.17 ± 0.73	9.12 ± 1.01	9.85 ± 0.74	5.38
643.4346	32:2	PtdOH	16:1/16:1	8.14 ± 1.25	8.02 ± 1.11	8.03 ± 0.84	8.11 ± 0.91	8.15 ± 0.78	8.16 ± 0.84	1.00
657.4503	33:2	PtdOH	16:1/c17:0	0.87 ± 0.21	5.17 ± 0.97	5.89 ± 0.42	8.42 ± 0.68	9.36 ± 1.19	10.58 ± 0.96	12.16
671.4660	34:2	PtdOH	c17:0/c17:0	0.11 ± 0.07	5.09 ± 0.84	6.01 ± 0.57	9.03 ± 1.01	13.25 ± 1.45	13.74 ± 1.48	124.91
788.5449	32:2	PtdCho	16:1/16:1	6.43 ± 0.86	6.37 ± 0.32	6.44 ± 0.66	6.49 ± 0.85	6.54 ± 0.62	6.53 ± 0.87	1.02
802.5606	33:2	PtdCho	16:1/c17:0	2.78 ± 0.57	5.68 ± 0.49	6.10 ± 0.49	8.04 ± 0.62	8.22 ± 0.83	8.47 ± 0.92	3.05
816.5763	34:2	PtdCho	c17:0/c17:0	0.10 ± 0.05	5.12 ± 0.51	6.79 ± 0.53	9.15 ± 0.94	10.31 ± 0.76	10.99 ± 1.12	109.90
686.4768	32:2	PtdEtn	16:1/16:1	100.00 ± 1.64	98.57 ± 1.83	98.17 ± 1.76	97.44 ± 1.57	97.25 ± 1.86	97.09 ± 1.44	0.97
700.4925	33:2	PtdEtn	16:1/c17:0	12.19 ± 1.12	41.38 ± 1.97	42.16 ± 1.24	64.38 ± 1.98	68.41 ± 1.45	74.13 ± 1.69	6.08
714.5082	34:2	PtdEtn	c17:0/c17:0	1.49 ± 0.51	6.29 ± 0.73	7.53 ± 0.69	22.11 ± 0.17	25.85 ± 1.19	26.24 ± 1.82	17.61
717.4714	32:2	PtdGro	16:1/16:1	5.71 ± 0.92	6.93 ± 0.62	7.02 ± 0.87	6.78 ± 0.86	6.83 ± 0.78	7.18 ± 0.76	1.26
731.4871	33:2	PtdGro	16:1/c17:0	2.75 ± 0.72	5.15 ± 0.74	6.63 ± 0.91	8.24 ± 0.75	8.86 ± 0.68	9.31 ± 0.85	3.39
745.5028	34:2	PtdGro	c17:0/c17:0	0.08 ± 0.05	5.18 ± 0.58	6.34 ± 0.46	11.47 ± 0.99	11.69 ± 0.91	12.09 ± 0.83	151.13
805.4871	32:2	PtdIns	16:1/16:1	4.29 ± 0.79	4.43 ± 0.61	4.51 ± 0.53	4.37 ± 0.54	4.72 ± 0.62	4.90 ± 0.61	1.14
819.5027	33:2	PtdIns	16:1/c17:0	1.52 ± 0.62	4.18 ± 0.57	5.14 ± 0.48	5.08 ± 0.53	6.00 ± 0.79	6.36 ± 0.76	4.18
833.5183	34:2	PtdIns	c17:0/c17:0	0.06 ± 0.04	2.47 ± 0.32	2.82 ± 0.26	7.35 ± 0.61	8.17 ± 0.95	8.25 ± 0.66	137.50
730.4663	32:2	PtdSer	16:1/16:1	3.86 ± 1.53	3.72 ± 0.45	3.65 ± 0.45	3.51 ± 0.47	3.42 ± 0.56	3.26 ± 0.39	0.84
744.4819	33:2	PtdSer	16:1/c17:0	1.35 ± 0.76	3.14 ± 0.74	3.67 ± 0.58	3.70 ± 0.58	4.07 ± 0.43	4.24 ± 0.48	3.14
758.4975	34:2	PtdSer	c17:0/c17:0	0.14 ± 0.09	2.17 ± 0.34	2.86 ± 0.40	4.24 ± 0.46	4.72 ± 0.74	5.50 ± 0.83	39.29

[a] Et, ethanol; G, glycerol; DCF, diclofenac

[b] Abundance of molecular species is relative to the base peak (at m/z 686.4768, i.e. molecular species of 16:1/16:1-PE), which is arbitrarily determined to be 100%

[c] Mean ± S.D. from three measurements

Ptd_2Gro, is described in the Supplements. In addition, only tandem MS analysis of the two less common classes of phospholipids, i.e. acyl-PtdGro and *N*-acyl-PtdEtn, is described below.

Acyl-phosphatidylglycerol (acyl-PtdGro)

In the tandem MS, 1-palmitoyl-2-palmitoleoyl glycero-3-phospho-(3′-9,10-methylenehexadecanoyl)-1′-*sn*-glycerol (c17:0-16:0/16:1)-PtdGro at m/z 969.7165 has dominant carboxylic anions at m/z 255.2330 (16:0), m/z 253.2173 (16:1) and m/z 267.2330 (c17:0) (Fig. 3). Expanded m/z range between 700 and 750 is shown in Fig. 4. The abundance of $RCOO^-$ decreases in the order $R_2COO^- > R_3COO^- > R_1COO^-$, the abundance of R_2COO^- (16:1) being about twice the abundance of R_1COO^- (16:0). From the various abundance values of R_xCOO^- ions, the position of acyls in the acyl-PtdGro molecule can be determined based on known rules (Hsu et al. 2004). Further confirmation of the structure was possible on the basis of the ions generated by the loss of acyl ketenes, i.e. ions at m/z 719.4869 ($[M\text{-}H\text{-}C_{15}H_{31}CH{=}C{=}O]^-$), m/z 733.5025 ($[M\text{-}H\text{-}C_{14}H_{27}CH{=}C{=}O]^-$ and m/z 731.4869 ($[M\text{-}H\text{-}C_{14}H_{29}CH{=}C{=}O]^-$), arising from the loss of c17:0, 16:1 and 16:0 or from ions at m/z 969.7165.

The fatty acyl substituents are also reflected in the fragment ions at m/z 701.4763 (neutral loss of sn-3′ RCOOH group from [M-H]-), 715.4919 (neutral loss of sn-2 RCOOH group from [M-H]-) and 713.4763 (neutral loss of sn-1 RCOOH group from [M-H]-), respectively; these ions are formed by neutral loss of FA from [M–H]–. The preferential formation of an ion by loss of 16:1-ketene over the formation of an ion via loss of 16:1-acid is similar to the trend observed for PtdGro (Hsu and Turk 2005) and the substituent at *sn-2* is palmitoleyl. In addition, a pair of unique ions at m/z 421.2361 and their dehydrated product at m/z 403.2255 were identified, which fully confirms the presence of c17:0 at the *sn*-3′ position. The ion at m/z 391.2255 ($[M\text{-}H\text{-}R'_2CH{=}C{=}O\text{-}74\text{-}R'_3COOH]^-$) is more abundant than the ion at m/z 403.2255 ($[M\text{-}H\text{-}R'_{2(1)}COOH]^-$), which is again more abundant than the ion at m/z 389.2098 ($[M\text{-}H\text{-}R'_3CH{=}C{=}O\text{-}74\text{-}R_2COOH]^-$). For these reasons, it can be inferred that this molecular species has 16:0 and 16:1-acyls at the *sn*-1 and *sn*-2 positions of the glycerol backbone and the remaining position (*sn*-3′) is occupied by c17:0 acid.

The structure of the FA with a cyclopropane ring but not with a double bond was demonstrated both by analysis of 3-pyridylcarbonyl esters (formerly called picolinyl esters) by GC-MS and by reference (Santos et al. 2018). The region of lower molecular weight features typical ions, i.e. at m/z 92, 108, 151, 164, etc., for 3-pyridylcarbonyl esters. In the mass spectrum, there were two abnormalities, see Fig. 2S. First, the ion $[M\text{-}1]^+$ is more abundant than $[M]^+$ ion and second, an odd-numbered ion (the odd value of the ion in the mass spectrum of 3-pyridylcarbonyl esters is very unusual) i.e. ion at m/z 245, represents cleavage of the cyclopropane ring. Based on this mass spectrum, we assume the structure of FA with cyclopropane ring but no double bond, i.e. 9,10-methylene hexadecanoic acid (c17:0) and not heptadecenoic acid (17:1).

N-acyl-phosphatidylethanolamine (*N*-acyl-PtdEtn)

In the case of *N*-acyl-PtdEtn, two ions at m/z 255.2330, m/z 253.2173 and the precursor ion at m/z 938.7219 were identified as the majority ions, whereas the ion at m/z 267.2328 was not found (Fig. 5). Based on HRMS, it can be assumed that the

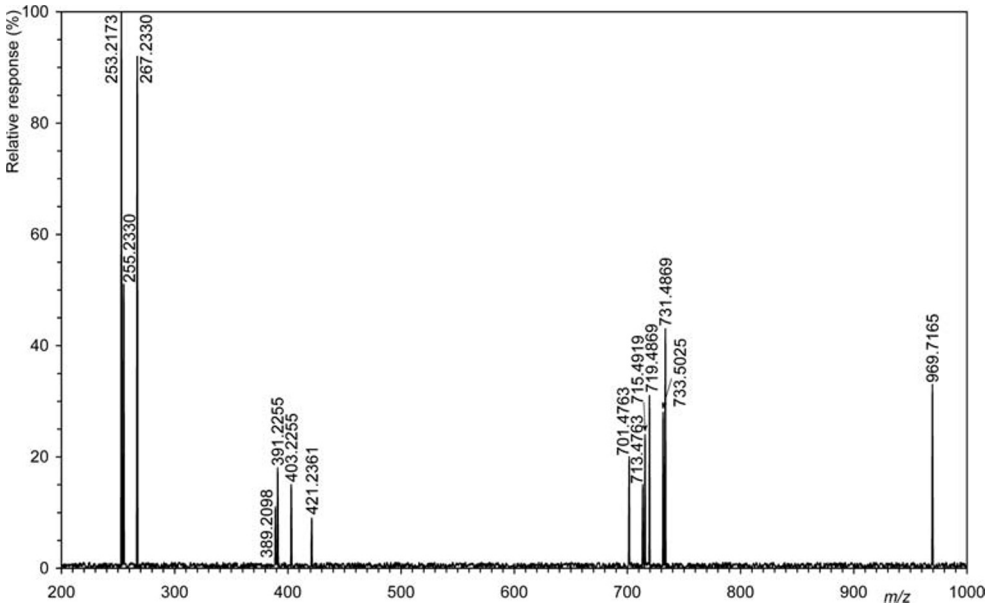

Fig. 3 Negative ion electrospray tandem mass spectrum of deprotonated of c17:0-16:0/16:1-PtdGro ((*Z*)-2-(hexadec-9-enoyloxy)-3-(hexadecanoyloxy)propyl 3-(8-(2-hexylcyclopropyl)octanoyloxy)-2-hydroxypropyl phosphate) from *Raoultella* sp. KDF8

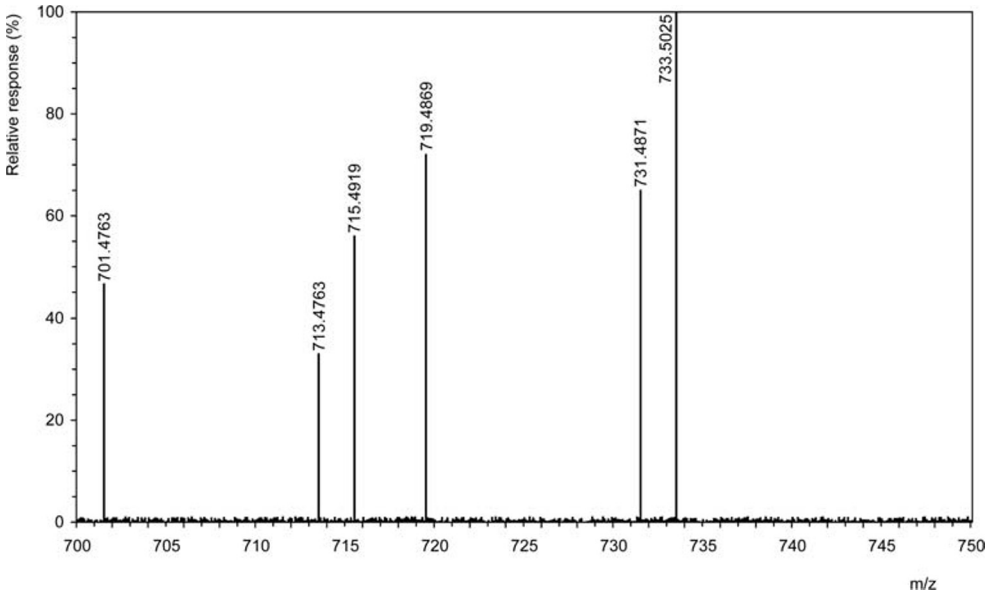

Fig. 4 The expanded mass spectrum in the range between 700 and 750 Da

acyl-PtdEtn contained palmitic, palmitoleic and c17:0 acids. In the tandem MS, cleavage involves the loss of $C_{16}H_{31}CONHCH_2CH_2$ and further acyls (loss of sn-2 acyl and loss of sn-1 acyl) to form two ions, i.e. those at m/z 391.2255 (summary formula $C_{19}H_{36}O_6P^-$) and at m/z 389.2337 (summary formula $C_{19}H_{34}O_6P^-$). The presence of c17:0 acid in the amide form was further confirmed by the presence of an ion at m/z 446.2677 (theoretical value for $C_{22}H_{41}NO_6P$ is 446.2671, Δ 0.6 mmu). Furthermore, the ions $[M\text{-}R_1COOH]^-$ and $[M\text{-}R'_2CH{=}C{=}O]$ were identified at m/z 682.4817 and at m/z 702.5079. They are formed due to neutral loss of fatty acids and ketenes from *sn*-1 and *sn*-2 positions of the glycerol backbone. The values for $[M\text{-}R_1COOH]^-$ (682.4817), $[M\text{-}R_1CH{=}C{=}O]^-$ (700.4923), $[M\text{-}R_2COOH]^-$ (684.4974) and $[M\text{-}R_2CH{=}C{=}O]^-$ (702.5079) ions were obtained. Ions at m/z 702.5079, which result from a loss of ketene ($C_{14}H_{27}CH{=}C{=}O$) from 16:1 acid, were far more abundant than the ion at m/z 700.4923 resulting from the loss of ketene from *sn*-1, suggesting the structure of the *N*-c17:0-16:0/16:1-PtdEtn according to already published data (Hsu and Turk 2009). This also corresponds to the abundance ratio of acyls, i.e. 16:0 (sn-1)/16:1 (sn-2) that approaches 1:2, see also Holmback et al. (2001).

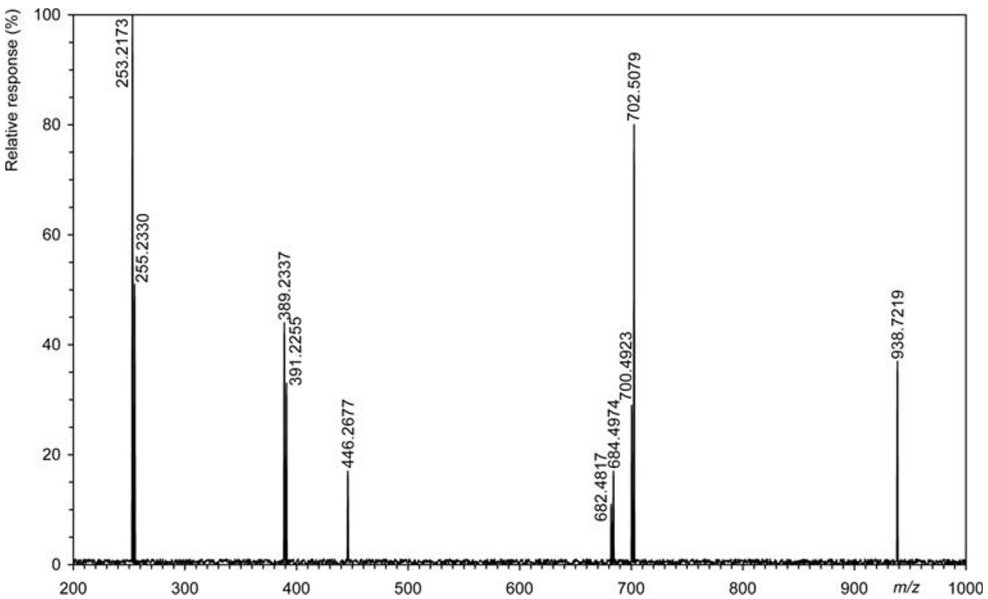

Fig. 5 Negative ion electrospray tandem mass spectrum of deprotonated of *N*-c17:0-16:0/16:1 PtdEtn ((*Z*)-2-(hexadec-9-enoyloxy)-3-(hexadecanoyloxy)propyl 2-(8-(2-hexylcyclopropyl)octanamido)ethyl phosphate) from *Raoultella* sp. KDF8

Discussion

Phospholipid analysis of bacteria has already been described many times, for example in the chapter of a book (Wardhan and Mudgal 2017). Our results are similar to previously reported results of TLC of phospholipids from different strains of *Acinetobacter radioresistens* (Luo et al. 2018) and *E. coli*, *Klebsiella oxytoca* and *K. pneumoniae* (Aluyi et al. 1992), which differ only in the abundances of phospholipid classes. The results of our semi-quantitative determination of phospholipid classes by TLC were not completely consistent with the results of ESI-MS lipid analysis. The quantitation by TLC used absorbance at 220 nm, while the abundance of ions formed by electrospray ionization was used for the analysis of phospholipids. It is therefore clear that two such totally different methods cannot give the same results.

Nevertheless, it is possible to gather from the measured values that the trends are the same. The separation of *N*-acyl-PtdEtn and acyl-PtdGro was not complete, which is also mentioned in a previous paper (Luo et al. 2018). All nine isolated classes of phospholipids are commonly present in gram-negative bacteria (Sohlenkamp and Geiger 2016). However, it should be noted that phospholipids with three acyls are less common (Yagüe et al. 2006). As described above for FA, the content of phospholipids also changes. Luo et al. (2018) found increasing *N*-acyl-PtdEtn content in cells (*Acinetobacter radioresistens*) in the stationary phase when carbon sources are already depleted. We compared the content of NAPtdEtn, or rather the ratio of two molecular species, i.e. 16:1/16:1/16:1 versus c17:0/c17:0/c17:0. This ratio was 1.79, representing 24 h of cultivation in ethanol, and increased to 3.91 (24 h, exponential growth phase) up to 4.85 (48 h, declining growth phase) during the incubation of the strain KDF8 in DCF. One of the problems that is common in the use of DCF is that aromatic rings are very poorly biodegradable. Many publications have reported on the metabolism or co-metabolism of DCF by various bacteria (Caracciolo et al. 2015; Palyzová et al. 2018), but the metabolites derived from aromatic rings have been rarely published. A recent study has proven the biodegradation of aromatic rings (Palyzová et al. 2019) with ^{13}C-labelled DCF. One of the reasons for the poor biodegradation of DCF may be its poor solubility in water, so its solutions in pure ethanol are also used.

Another problem with the biodegradation of DCF is its transport through biological membranes. Membrane fluidity may be affected by the variation in acyl chains, i.e. FA, as shown in Table 1. As mentioned earlier in the introduction, FA unsaturation, chain length and general FA composition differ depending on the cultivation of the bacteria on a given carbon source. Examples that can be generalized include a shift of monounsaturated FA content to cyclo FA (Ingram et al. 1978; Shabala and Ross 2008). The influence of the composition of the culture medium, or rather the carbon source, was manifested both in the exponential and in the stationary phase. The fatty acid content of the 24-h ethanol culture and the 24- and 48-h fatty acid content of the DCF culture are different, see Table 1. For example, the ratio of 16:1 to c17:0 in a 24-h culture on ethanol, i.e. in exponential phase, is 1.26 while at the same time in DCF (again exponential phase) cultivation, it was 2.59. The ratio increases with time, so the effect of DCF was fully manifested after 48 h (declining growth phase) and was 2.97. These values indicate that the effect of DCF on cell lipids is beginning to appear in the exponential phase. Poger and Mark (2015) used artificially prepared lipid bilayers from PtdCho derivatives that had in the *sn*-2 position ester-bound palmitic acid and in the *sn*-1 position, e.g. palmitoleoyl or *cis*-9,10-methanopalmitoyl chains. Lateral diffusion coefficients of 16:1/16:0-PtdCho and *cis*-c16:0/16:0-PtdCho differed and had values of 2.8 and 3.2 μm^2/s, respectively. Based on these values, the authors found that cyclopropanoic FA increases plasma membrane fluidity while inducing a more ordered state within hydrocarbon chains compared to unsaturated FA. This increases membrane stability while reducing its permeability to toxic compounds.

The effect of different sources of carbon on cell membrane FA composition of the strain *Klebsiella planticola* DSZ was described by Sánchez et al. (2005). Membrane FA analysis showed that the strain DSZ adapted to growth on the toxic organic compound simazine used as a source of carbon by increasing the degree of saturation of FA. Additionally, in our case (Table 1), the sum of c17:0 increased by about one order in the 72-h culture on DCF versus the 24-h glycerol culture in stationary growth phase.

Although descriptions of the effect of DCF on mammalian (human) and bacterial cells, e.g. inhibition of the prostaglandin-endoperoxide synthase-2 also known as cycloxygenase-2 (Cryer and Feldman 1998), have already been published several times, its effect on bacteria has not been fully investigated. This is evidenced, for example, by the work describing the activity of DCF with streptomycin against *Mycobacterium tuberculosis* (Dutta et al. 2007).

Other authors (Broniatowski et al. 2015) used anionic phospholipid Langmuir monolayers composed of 16:0/18:1-PtdEtn and two phospholipids (PtdGro and Ptd$_2$Gro) isolated from *E. coli*, i.e. phospholipids that contain at least one cyclopropane ring in the molecule. Interactions of cell monolayers with pentacyclic triterpenes (ursane series) have shown disorganizing effects on the model membrane, where the free energy of mixing (ΔG^{exc}) showed large positive changes. Based on these facts, it can be said that pentacyclic triterpenes are incorporated into the membrane and thus interfere with the formation of a hydrogen bond between the polar heads of PtdEtn and PtdGro, and also disrupt the arrangement of acyls

of phospholipids and alter the PtdEtn/PtdGro ratio at a particular site, i.e. the integrity of lipid rafts.

The same team (Broniatowski et al. 2016) again used artificially prepared Langmuir monolayers, bisphenols being used as xenobiotics. Unlike pentacyclic triterpenes, these substances are of an aromatic character and therefore, with their spatial orientation, they are much more similar to DCF, which is also composed of two aromatic rings. All bisphenols used interact with PtdGro and Ptd_2Gro from *E. coli*, where the main indicator of penetration into the monolayer is the hydrophobicity of bisphenols. This, of course, also depends on the hydrophobicity and stiffness of the membranes, causing significant changes in their structure and physical properties.

The interaction of thymol with a model membrane composed of 16:0/16:0-PtdCho has been investigated (Ferreira et al. 2016). It has been found that this aromatic compound expands PtdCho monolayers and decreases their surface elasticity and therefore changes the physico-chemical properties of bilayers. In another study (Suklabaidya et al. 2018), the antibiotic norfloxacin increased the biomembrane fluidity.

In our case, it is clear that DCF very strongly modulates membrane fluidity, as will be mentioned below. This fact was confirmed by the lipidomic analysis of several hundred molecular species of phospholipids (Table 1S) (Supplements).

Jasim et al. (2018) described the effect of polymyxin B antibiotic on the membrane of *Klebsiella* bacterium. Unfortunately, although the authors performed lipidomic analysis, they do not comment on the decline or growth of individual molecular species. However, based on their results (their Fig. 5), it can be deduced that, for example, 15:0/15:0-PtdEtn in polymyxin B-susceptible strains of *K. pneumoniae* FADDI-KP069 were changed less than 0.25-fold, whereas in resistant strains, the change was greater than 2-fold. Our results, see Tables 2 and 1S, clearly show that the change in the cell membranes structure of the *Raoultella* bacterium (formerly designated *Klebsiella,* Drancourt et al. 2001) is primarily due to the change in the presence of FA in phospholipids. The phospholipid content itself has a significant share in the change and their spatial layout is completely different. Table 2 shows the relative abundances in percent of individual peaks where 100% refers to the molecular species (PtdEtn 16:1/16:1; base peak) in glycerol cultivation. In the case of cultivation on diclofenac, see Table 1S in the Supplements, it was a base peak PtdEtn 18:1/18:1. Since the same molecular species measured on the same instrument are compared and the individual samples differ only in the type of cultivation, we did not use absolute values that are difficult to obtain and to quantify, mainly because of the impossibility of buying commercially available standards, e.g. APtdGro, NAPtdEtn, etc.

Further, pentachlorophenol, a water-soluble degradation product of many polychlorinated pesticides, has changed the structure of myristoyl PtdEtn, PtdGro and Ptd_2Gro in the microbial membrane model (Wojcik et al. 2018).

Therefore, we believe that *Raoultella* cells grown with DCF may alter their spatial orientation of phospholipids in the membrane, e.g. PtdEtn having double chains with unsaturated palmitoleic acid forming inverted cones changing to near-cylinders represented by molecular species with c17:0, i.e. having a critical packing parameter (CPP) closer to one (Wardhan and Mudgal 2017).

Conclusions

Since the PtdEtn content decreased and the content of phospholipids having three and four acyl chains (acyl-phosphatidylglycerol, *N*-acyl-phosphatidylethanolamine and cardiolipin) increased with increasing cultivation time in all cultures including those on difficult-to-utilize carbon sources, we assume that the cell membranes are destabilized. The cells try to compensate for this destabilization, at least according to our assumption, by altering the geometric arrangement of acyl chains. There was an increase of up to several orders of molecular species in which acyl chains were completely changed from monounsaturated FA to cyclopropane FA (16:1 versus c17:0). A 1750-fold increase in cardiolipin ratio of 16:1 to c17:0 acids can be mentioned as an extreme example.

Acknowledgments This research was supported by the Ministry of Education, Youth and Sports of the Czech Republic (LO1509) and the Epsilon programme of the Technology Agency of the Czech Republic (TH02030337).

Compliance with ethical standards

Conflict of interest The authors declare that they have no conflict of interest.

References

Aluyi HS, Boote V, Drucker DB, Wilson JM, Ling YH (1992) Analysis of polar lipids from some representative enterobacteria, *Plesiomonas* and *Acinetobacter* by fast atom bombardment-mass spectrometry. J Appl Microbiol 73:426–432

Bernat P, Siewiera P, Sobon A, Długonski J (2014) Phospholipids and protein adaptation of *Pseudomonas* sp. to the xenoestrogen tributyltin chloride (TBT). World J Microbiol Biotechnol 30:2343–2350

Bligh EG, Dyer WJ (1959) A rapid method of total lipid extraction and purification. Can J Biochem Physiol 37:911–917

Broniatowski M, Mastalerz P, Flasiński M (2015) Studies of the interactions of ursane-type bioactive terpenes with the model of *Escherichia coli* inner membrane-Langmuir monolayer approach. Biochim Biophys Acta 1848:469–476

Broniatowski M, Sobolewska K, Flasiński M, Wydro P (2016) Studies on the interactions of bisphenols with anionic phospholipids of decomposer membranes in model systems. Biochim Biophys Acta 1858: 756–766

Caracciolo AB, Topp E, Grenni P (2015) Pharmaceuticals in the environment: biodegradation and effects on natural microbial communities. A review. J Pharm Biomed Anal 106:25–36

Cryer B, Feldman M (1998) Cyclooxygenase-2 selectivity of widely used nonsteroidal anti-inflammatory drugs. Am J Med 104:413–421

Dembitsky VM, Rezanka T, Bychek IA (1992) Fatty-acids and phospholipids from lichens of the order *Lecanorales*. Phytochemistry 31: 851–853

Domaradzka D, Guzik U, Hupert-Kocurek K, Wojcieszynska D (2016) Toxicity of diclofenac and its biotransformation by *Raoultella* sp. DD4. Pol J Environ Stud 25:2211–2216

Drancourt M, Bollet C, Carta A, Rousselier P (2001) Phylogenetic analyses of *Klebsiella* species delineate *Klebsiella* and *Raoultella* gen. nov., with description of *Raoultella ornithinolytica* comb, nov., *Raoultella terrigena* comb. nov and *Raoultella planticola* comb. nov. Int J Syst Evol Microbiol 51:925–932

Duldhardt J, Gaebel L, Chrzanowski L, Nijenhuis I, Hartig C, Schauer F, Heipieper HJ (2010) Adaptation of anaerobically grown *Thauera aromatica*, *Geobacter sulfurreducens* and *Desulfococcus multivorans* to organic solvents on the level of membrane fatty acid composition. Microb Biotechnol 3:201–209

Dutta NK, Mazumdar K, Dastidar SG, Park JH (2007) Activity of diclofenac used alone and in combination with streptomycin against *Mycobacterium tuberculosis* in mice. Int J Antimicrob Agents 30:336–340

Ferreira JV, Capello TM, Siqueira LJ, Lago JH, Caseli L (2016) Mechanism of action of thymol on cell membranes investigated through lipid Langmuir monolayers at the air-water interface and molecular simulation. Langmuir 32:3234–3241

Han X, Gross RW (2003) Global analyses of cellular lipidomes directly from crude extracts of biological samples by ESI mass spectrometry: a bridge to lipidomics. J Lipid Res 44:1071–1079

Heipieper HJ, Meinhardt F, Segura A (2003) The cis-trans isomerase of unsaturated fatty acids in *Pseudomonas* and *Vibrio*: biochemistry, molecular biology and physiological function of a unique stress adaptive mechanism. FEMS Microbiol Lett 229:1–7

Holmback J, Karlsson AA, Arnoldsson KC (2001) Characterization of N-acylphosphatidylethanolamine and acylphosphatidylglycerol in oats. Lipids 36:153–165

Hsu FF, Turk J (2005) Electrospray ionization with low-energy collisionally activated dissociation tandem mass spectrometry of complex lipids: structural characterization and mechanisms of fragmentation. In: Byrdwell WC (ed) Modern methods for lipid analysis by liquid chromatography. AOCS Publishing, Urbana, pp 61–178

Hsu FF, Turk J (2009) Electrospray ionization with low-energy collisionally activated dissociation tandem mass spectrometry of glycerophospholipids: mechanisms of fragmentation and structural characterization. J Chromatogr B Anal Technol Biomed Life Sci 877:2673–2695

Hsu FF, Turk J, Shi Y, Groisman EA (2004) Characterization of acylphosphatidylglycerols from *Salmonella typhimurium* by tandem mass spectrometry with electrospray ionization. J Am Soc Mass Spectrom 15:1–11

Ingram LO (1977) Preferential inhibition of phosphatidyl ethanolamine synthesis in *E. coli* by alcohols. Can J Microbiol 23:779–789

Ingram LO, Ley KD, Hoffmann EM (1978) Drug-induced changes in lipid composition of *E. coli* and of mammalian cells in culture: ethanol, pentobarbital, and chlorpromazine. Life Sci 22:489–494

Jasim R, Han ML, Zhu Y, Hu X, Hussein MH, Lin YW, Zhou QT, Dong CYD, Li J, Velkov T (2018) Lipidomic analysis of the outer membrane vesicles from paired polymyxin-susceptible and -resistant *Klebsiella pneumonia* clinical isolates. Int J Mol Sci 19:2356

Knittelfelder OL, Weberhofer BP, Eichmann TO, Kohlwein SD, Rechberger GN (2014) A versatile ultra-high performance LC-MS method for lipid profiling. J Chromatogr B Anal Technol Biomed Life Sci 951–952:119–128

Luo Y, Javed MA, Deneer H, Chen X (2018) Nutrient depletion-induced production of tri-acylated glycerophospholipids in *Acinetobacter radioresistens*. Sci Rep 8:7470

Meerburg F, Hennebel T, Vanhaecke L, Verstraete W, Boon N (2012) Diclofenac and 2-anilinophenylacetate degradation by combined activity of biogenic manganese oxides and silver. Microb Biotechnol 5:388–395

Moreira IS, Bessa VS, Murgolo S, Piccirillo C, Mascolo G, Castro PML (2018) Biodegradation of diclofenac by the bacterial strain *Labrys portucalensis* F11. Ecotoxicol Environ Saf 152:104–113

Novak J, Sokolova L, Lemr K, Pluhacek T, Palyzova A, Havlicek V (2017) Batch-processing of imaging or liquid-chromatography mass spectrometry datasets and de novo sequencing of polyketide siderophores. Biochim Biophys Acta 1865:768–775

Palyzová A, Zahradník J, Marešová H, Sokolová L, Kyslíková E, Grulich M, Štěpánek V, Řezanka T, Kyslík P (2018) Potential of the strain *Raoultella* sp. KDF8 for removal of analgesics. Folia Microbiol 63: 273–282

Palyzová A, Marešová H, Zahradník J, Řezanka T (2019) Characterization of the catabolic pathway of diclofenac in *Raoultella* sp. KDF8. Int Biodeterior Biodegradation 137:88–94

Perly B, Smith ICP, Jarrell HC (1985) Effects of the replacement of a double bond by a cyclopropane ring in phosphatidylethanolamines: a 2H NMR study of phase transitions and molecular organization. Biochemistry 24:1055–1063

Poger D, Mark AE (2015) A ring to rule them all: the effect of cyclopropane fatty acids on the fluidity of lipid bilayers. J Phys Chem B 119: 5487–5495

Radjenovic J, Petrovic M, Barcelo D (2009) Fate and distribution of pharmaceuticals in wastewater and sewage sludge of the conventional activated sludge (CAS) and advanced membrane bioreactor (MBR) treatment. Water Res 43:831–841

Sánchez M, Garbi C, Martínez-Álvarez R, Ortiz LT, Allende JL, Martín M (2005) *Klebsiella planticola* strain DSZ mineralizes simazine: physiological adaptations involved in the process. Appl Microbiol Biotechnol 66:589–596

Santos IC, Smuts J, Choi WS, Kim Y, Kim SB, Schug KA (2018) Analysis of bacterial FAMEs using gas chromatography-vacuum ultraviolet spectroscopy for the identification and discrimination of bacteria. Talanta 182:536–543

Segura A, Duque E, Mosqueda G, Ramos JL, Junker F (1999) Multiple responses of Gram-negative bacteria to organic solvents. Environ Microbiol 1:191–198

Shabala L, Ross T (2008) Cyclopropane fatty acids improve *Escherichia coli* survival in acidified minimal media by reducing membrane permeability to H+ and enhanced ability to extrude H^+. Res Microbiol 159:458–461

Sohlenkamp C, Geiger O (2016) Bacterial membrane lipids: diversity in structures and pathways. FEMS Microbiol Rev 40:133–159

Suklabaidya S, Debnath P, Dey B, Bhattacharjee D, Hussain SA (2018) Interaction of an antibiotic—norfloxacin with lipid membrane. Mater Today Proc 5:2373–2380

Vancura A, Rezanka T, Marsálek J, Melzoch K, Basarova G, Kristan V (1988) Metabolism of L-threonine and fatty-acids and tylosin biosynthesis in *Streptomyces fradiae*. FEMS Microbiol Lett 49:411–415

Wardhan R, Mudgal P (2017) Textbook of membrane biology. Springer Nature, London

Wojcik A, Pawlowski M, Wydro P, Broniatowski M (2018) Effects of polychlorinated pesticides and their metabolites on phospholipid organization in model microbial membranes. J Phys Chem B 122: 12017–12030

Yagüe G, Segovia M, Valero Guillén PL (2006) Acyl phosphatidylglycerol: a major phospholipid of *Corynebacterium amycolatum*. FEMS Microbiol Lett 151:125–130